Applied Surface Science 419 (2017) 692–696

Contents lists available at ScienceDirect

Applied Surface Science

journal homepage: www.elsevier.com/locate/apsusc

Short Communication

Self-assembled thin films of Fe_3O_4-Ag composite nanoparticles for spintronic applications

Chengpeng Jiang[a], Chi Wah Leung[b], Philip W.T. Pong[a,*]

[a] Department of Electrical and Electronic Engineering, University of Hong Kong, Hong Kong
[b] Department of Applied Physics, Hong Kong Polytechnic University, Hong Kong

ARTICLE INFO

Article history:
Received 3 April 2017
Received in revised form 10 May 2017
Accepted 13 May 2017
Available online 15 May 2017

Keywords:
Interfacial assembly
Material interface
Magnetic nanoparticle
Nanoparticle thin film
Magnetoresistance
Spintronics

ABSTRACT

Controlled self-assembly of multi-component magnetic nanoparticles could lead to nanomaterial-based magnetic devices with novel structures and intriguing properties. Herein, self-assembled thin films of Fe_3O_4-Ag composite nanoparticles (CNPs) with hetero-dimeric shapes were fabricated using interfacial assembly method. The CNP-assembled thin films were further transferred to patterned silicon substrates followed by vacuum annealing, producing CNP-based magnetoresistive (MR) devices. Due to the presence of intra-particle interfaces and inter-particle barriers, an enhanced MR ratio and a non-linear current-voltage relation were observed in the device. The results of this work can potentially pave the way to the future exploration and development of spintronic devices built from composite nanomaterials.

1. Introduction

The controlled organizations of magnetic nanoparticles with discrete energy levels into ordered nanostructures (such as one-dimensional chains, two-dimensional films, or three-dimensional superlattices) [1–5] are of great value for bottom-up fabrication of magnetic materials and devices. Compositions and morphology of the constituent nanoparticles as the building blocks can be finely tailored, enabling us to tune their collective properties as desired [6,7]. In particular, the self-assembly of multi-component magnetic nanoparticles into well-defined nanostructures has attracted considerable interests, since it provides a promising way to utilize the spin-dependent effects arising from the interfaces and interactions of the constituent components. Currently, several variants of the self-assembly methods (field-assisted assembly, confined-space assembly, interfacial assembly) [8–12] have been reported for constructing magnetic materials and devices using binary or ternary nanoparticles [7,13,14]. However, the controlled assembly of composite nanoparticles (CNPs) into ordered magnetic nanostructures with uniform properties has been scarcely attempted. Although challenging, the ability to fabricate CNP-assembled nanostructures is important for developing future spintronic devices built from composite nanomaterials. It is anticipated that such CNP-based spintronic devices could exhibit intriguing features compared with their binary counterparts, due to the distinctive interface and surface structures of the former.

As an example of composite nanoparticles, magnetic-metallic Fe_3O_4-Ag nanoparticles have attracted wide attentions due to their great potential for spintronic applications. Magnetite Fe_3O_4, as a ferromagnetic material with a favorable Curie temperature (860 K), shows high spin polarization and half-metallic behavior due to electron hopping between different iron ions at room temperature [15]. On the other hand, silver is regarded as an excellent conducting material with the highest conductivity. Several groups have reported the magnetoresistance (MR) measurement of composite Fe_3O_4-Ag systems [16–19]. These works mainly focus on granular materials formed as polycrystalline films, compacted powers, or cluster assemblies. For the purpose of investigating the physical properties and transport behaviors of Fe_3O_4-Ag CNPs, a nanoparticle-based system with well-defined particle arrangement and material interface needs to be fabricated.

Herein, this work presents the self-assembly of Fe_3O_4-Ag CNPs with hetero-dimeric shapes by an improved interfacial assembly technique. Uniform thin films composed of orderly assembled CNPs were produced and further transferred to silicon substrates patterned with electrodes. The vacuum annealing treatment and the resulting close packing of the CNPs allows the measurement of their magnetoresistance (MR), leading to CNP-based magnetoresistive

* Corresponding author. Tel.: +852 2857 8491; fax: +852 2559 8738.
E-mail address: ppong@eee.hku.hk (P.W.T. Pong).

http://dx.doi.org/10.1016/j.apsusc.2017.05.116
0169-4332/

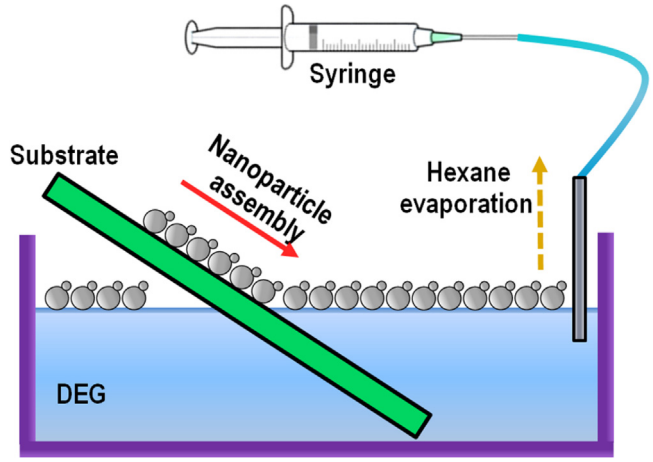

Fig. 1. Schematic illustration of the self-assembly method at liquid-air interface.

devices. Magneto-transport and electron-transport studies of the device were performed, and the results indicate that the Fe_3O_4-Ag CNPs can be exploited for spintronic applications.

2. Material and methods

Fe_3O_4-Ag CNPs were obtained by a seed-mediated synthesis protocol, in which Fe_3O_4 nanoparticles provide the nucleation sites for the growth of Ag nano-grain under mild reaction conditions [20]. At first, 10-nm Fe_3O_4 nanoparticles were obtained by thermal decomposition of iron-oleate complex following published procedures [21]. The Fe_3O_4 nanoparticles were purified twice by acetone-induced precipitation and dispersed in toluene. Afterwards, silver acetate (0.6 mmol) dissolved in oleylamine (18 mmol) was quickly injected into the toluene solution (60 mL) of Fe_3O_4 nanoparticles (0.45 mmol based on Fe) preheated at 80 °C. This hot-injection technique promotes the reduction of Ag^+ ions and condensation of Ag atoms on Fe_3O_4 seeds [20]. The reaction mixture was vigorously stirred and kept at 85 °C for 2 h under N_2. The product was extensively purified by ethanol-induced precipitation and redispersed in hexane.

Self-assembly of the Fe_3O_4-Ag CNPs was achieved by depositing them from liquid-air interface onto solid substrates by an improved evaporation-induced approach [13], as schematically illustrated in Fig. 1. Typically, 10 μL hexane solution of Fe_3O_4-Ag CNPs was gently spread over the surface (300 mm^2) of diethylene glycol (DEG) stored in a plastic pill box. The pill box was covered by a glass slide and the hexane was allowed to evaporate in a controlled manner, producing a floating thin film of CNPs supported on the DEG surface. By withdrawing the DEG using a syringe pump at a constant rate, this CNP-assembled thin film was transferred to a Si substrate (200 nm thermally oxidized surface) patterned with 30 nm thick Au electrodes. The sample was annealed in vacuum at 400 °C for 1 h to remove adsorbed organic molecules and reduce inter-particle distance [13].

3. Results and discussion

The transmission electron microscopy (TEM) image in Fig. 2a reveals that the as-synthesized Fe_3O_4-Ag CNPs are monodisperse and they are in hetero-dimeric shape. The average sizes of the small and the large nano-grains are 3 nm and 10 nm respectively. The CNPs organized into a monolayer at low concentrations (Fig. 2a, TEM) and they formed as a closely packed multilayer at high concentrations (Fig. 1a inset, SEM). The measured lattice spacing based on the selected area electron diffraction (SAED) patterns of the CNPs in Fig. 2b can be well indexed to magnetite (JCPDS #19-0629) and crystalline silver phases (JCPDS #65-2871), confirming that the composition of the CNP is Fe_3O_4-Ag. By measuring the lattice fringes from the high-resolution TEM image in the inset of Fig. 2b, it can be inferred that the small-sized Ag nano-grain is attached on the surface of the large-sized Fe_3O_4 nano-grain and their interfacial region is well preserved. As shown in Fig. 2c, hysteresis loop (MH curve) of the CNPs in solid form was measured to study their magnetic properties. A small coercivity (H_c) of 0.69 Oe was recorded and the low-field MH curve exhibits nearly linear responses to applied magnetic field due to the superparamagnetic contribution of the Fe_3O_4 nano-grains with single domain behavior [22,23]. The Fe_3O_4-Ag CNPs show a saturation magnetization (M_s) of 26.0 emu/g, which is lower than that of bulk Fe_3O_4 (84.5 emu/g). Such a decrease of M_s in our case is due to the synergistic results of surface spin canting, lattice strain effect, and the presence of non-magnetic Ag nano-grains [22]. As presented in Fig. 2d, ultraviolet-visible (UV–vis) spectrum of the CNPs dissolved in toluene was acquired to investigate their plasmonic properties. Compared with pure Fe_3O_4 nanoparticles, the Fe_3O_4-Ag CNPs demonstrate a strong absorbance peak at 421 nm, which arises from the surface plasmon resonance of the Ag nano-grains. Differential scanning calorimetry (DSC) curve of the CNPs in powder form was obtained to study their thermal properties, and the results are presented in Fig. 2e. Two endothermic peaks at high temperature (275 °C and 407 °C) were observed, implying that the capping ligands covalently bound on the surface of the CNP may have two different binding strengths [24]. DSC analysis also indicates that the heat treatment at 400 °C could effectively remove most of the organics. All the characterization results of the CNPs reveal that the obtained nanoparticles contain both magnetic and metallic nano-grains, and they were stabilized by organic capping ligands.

By depositing the CNP-assembled thin films onto patterned SiO_2/Si substrates using the interfacial assembly technique [11], CNP-based magnetoresistive devices were fabricated, as schematically illustrated in Fig. 3a. The optical micrograph in Fig. 3b shows that a continuous thin film fully covers the substrate surface over hundreds of microns. The atomic force microscopy (AFM) image of the CNP-assembled thin film is presented in Fig. 3c. The root-mean-square roughness of the thin film was 4.6 nm, and it reveals that the thin film is smooth at nanoscale and its roughness could be attributed to different spatial arrangement of the Fe_3O_4-Ag hetero-dimeric nanoparticles. Besides, the thickness of the thin film (determined by scanning from coated region to uncoated region) was 23.0 nm, and it indicates that approximately two layers of the Fe_3O_4-Ag hetero-dimeric nanoparticles were deposited onto the substrate surface, considering that each nanoparticle is composed of a 10 nm magnetite nano-grain and a 3 nm silver nano-grain. The SEM image in Fig. 3d shows that the CNPs were closely packed together without any obvious vacancy or crack. Besides, a few spherical nano-grains sized at ~12 nm with brighter colors were observed, as shown in the inset of Fig. 3d, and they may be formed due to the sintering and coalescing of excessive Ag nano-grains during the annealing process. SEM elemental mappings for Ag and Fe obtained by scanning the region in Fig. 3d are presented in Fig. 3e and f respectively. The mappings demonstrate that both Ag and Fe distribute evenly in the thin film, confirming that the Fe_3O_4-Ag CNPs were uniformly deposited on the substrate. The characterization results above exhibit that the CNP-assembled thin film is continuous and smooth. It is believed that CNPs of other materials or other sizes can also be constructed into homogeneous thin films with nanoscale thickness using the same fabrication procedures. Besides, the stoichiometric composition calculated from energy-dispersive X-ray spectroscopy (EDX) analysis is $(Fe_3O_4)_{0.58}(Ag)_{0.42}$, indicating that the Fe content is rich in this thin film due to the large size of the magnetic component in the CNP.

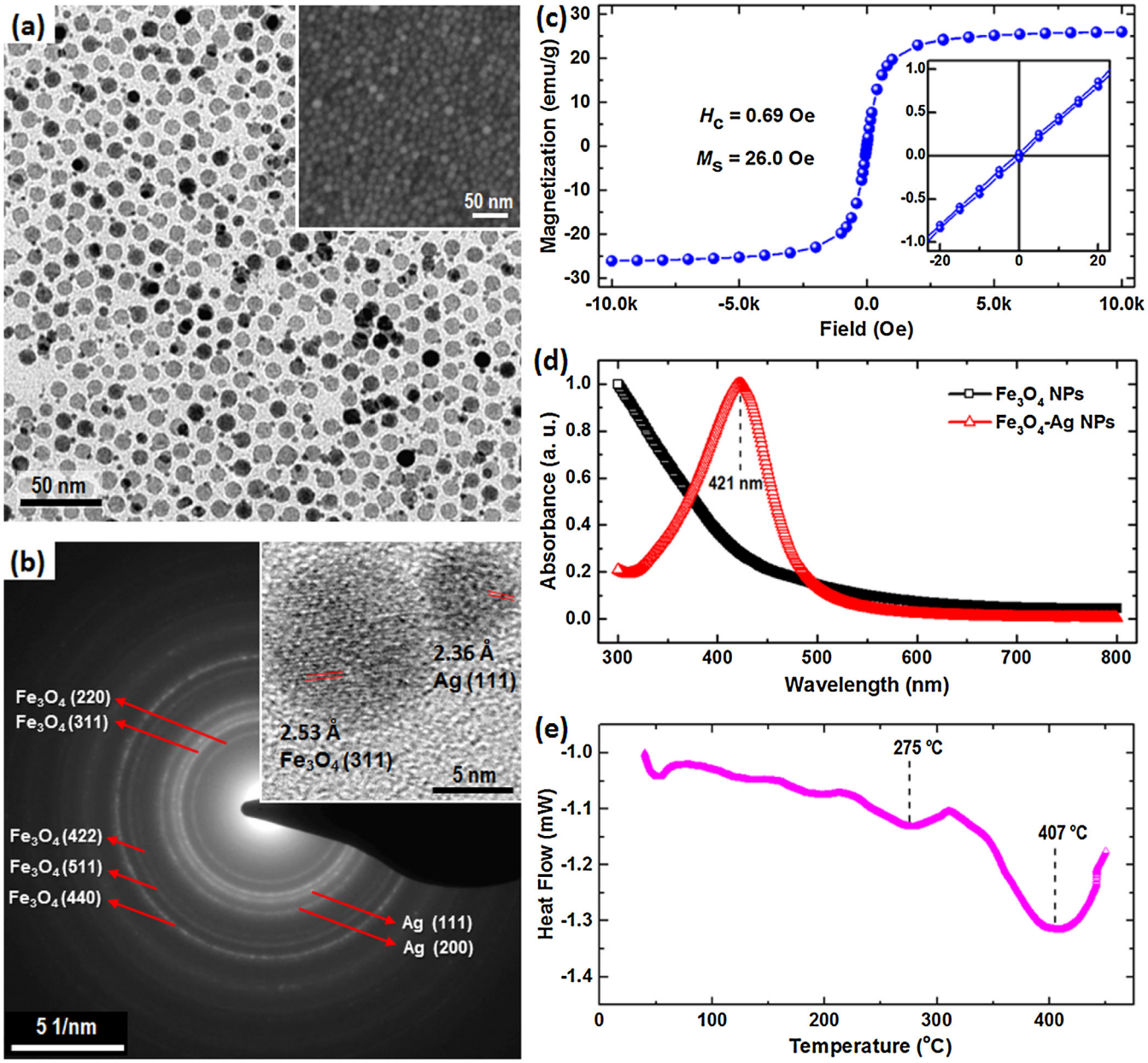

Fig. 2. (a) TEM image (inset: SEM image), (b) SAED patterns (inset: high-resolution TEM image), (c) MH curve (inset: enlarged view), (d) UV–vis spectra, and (e) DSC curve of the Fe_3O_4-Ag CNPs.

Magnetoresistance behavior of the CNP-based magnetoresistive device was investigated to study its magneto-transport properties. MR curve measured at 290 K in a current-parallel-to-field configuration (at a constant current of 0.85 μA) is presented in Fig. 4a. The negative magnetoresistance observed in this curve is presumably associated with the inter-particle and inter-grain transport of spin-polarized electrons [13,15,17,25], and the magnetoresistance is increased under higher applied magnetic field. An MR ratio of −2.2% at 1 T was recorded for the thin film assembled from the Fe_3O_4-Ag CNPs, and this value is larger than that (−1.8% at 1 T) of the superlattice membrane built from Fe_3O_4 nanoparticle (with particle size and film thickness comparable to ours) as reported in literature [13]. It should be noted that, in the Fe_3O_4 nanoparticle membrane, the interspace between adjacent Fe_3O_4 nanoparticles provide high-resistance tunneling barriers for the spin-polarized electrons. However, in the Ag–Fe_3O_4 nanoparticle thin film, the spin-polarized electrons not only tunnel through the inter-particle barriers among Ag–Fe_3O_4 nanoparticles but also scatter at the granular interfaces between Ag nano-grain and Fe_3O_4 nano-grain [16,25]. Therefore, the enhancement of the MR ratio observed in our case can be probably attributed to the additional spin-dependent scattering at the Ag–Fe_3O_4 granular interfaces and the enhanced spin-polarized tunneling across the inter-particle barriers. At high-field regions, the MR ratio shows no saturation and reaches −3.6% at 1.8 T. It is anticipated that a higher MR ratio could be achieved by optimizing the particle size and particle arrangement in the CNP-assembled thin film. The room-temperature MR measurement results of the CNP-based magnetoresistive device indicate that the Fe_3O_4-Ag CNPs, as a magnetic-metallic composite nanomaterial, are promising for constructing spintronic devices with high spin polarization and large magnetoresistance.

Current-voltage relation of the CNP-based magnetoresistive device was investigated to study its electron-transport properties. I–V curve recorded at 290 K under zero magnetic field where the

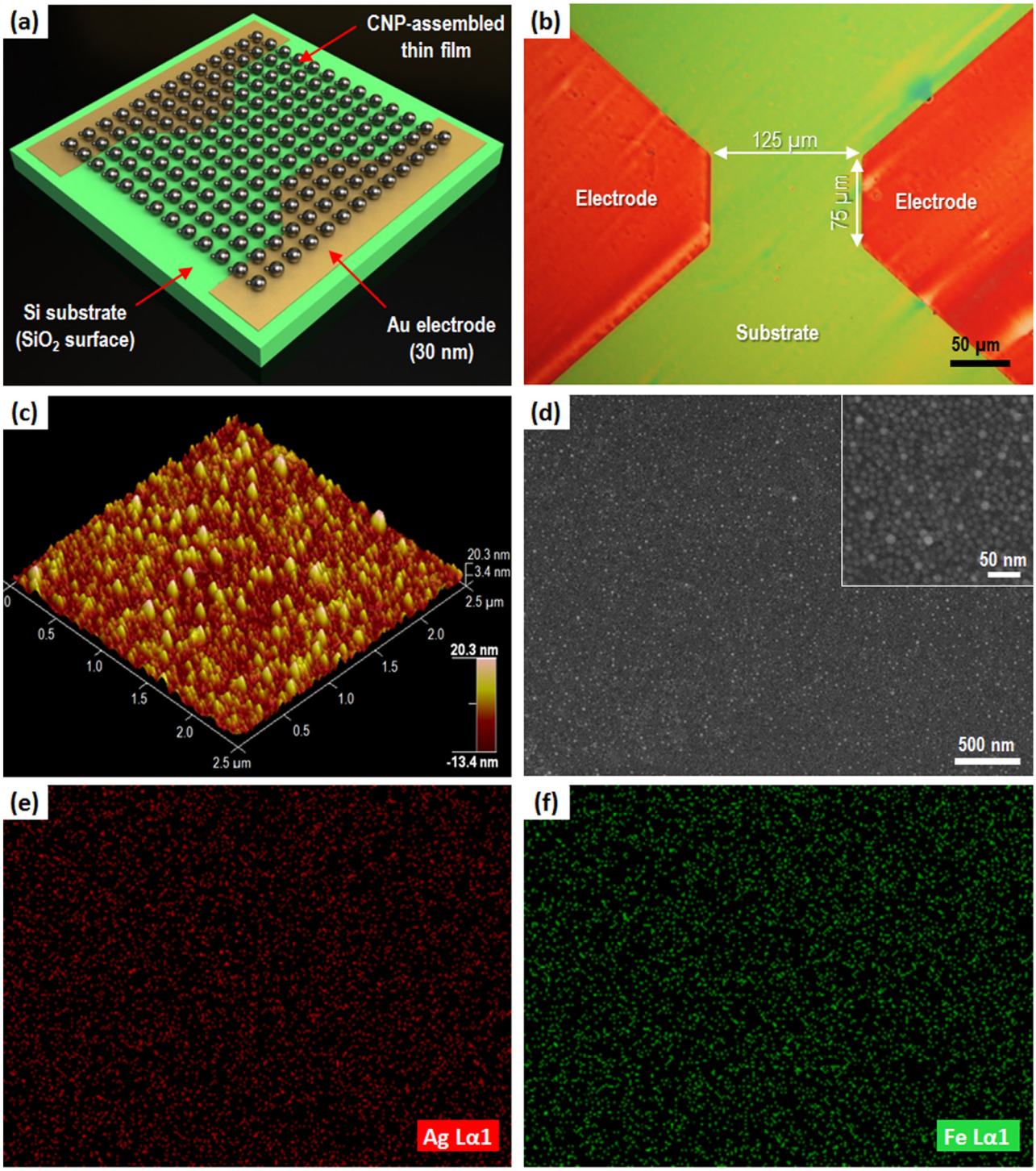

Fig. 3. (a) Schematic of the device structure. (b) Optical micrograph, (c) AFM image, (d) SEM image (inset: magnified view), and SEM-EDX elemental mapping for (e) Ag and (f) Fe of the CNP-assembled thin film in this device.

resistivity reaches maximum is presented in Fig. 4b. The I–V curve exhibits sigmoidal shapes with higher resistances at small voltages. The current flow for positive bias is similar to the negatively biased case. Fitting to the Simmons tunneling model for molecular tunnel junctions [26] gives a barrier height of 6.8 eV and a barrier thickness of 1.6 nm, which are plausible parameters. The nonlinear characteristic of the I–V curve indicates that the electron transport behavior could be possibly attributed to either direct electron tunneling across the inter-particle barriers formed by residual organic surfactants or field-dependent electron hopping among Fe^{3+} and Fe^{2+} ions within the magnetic Fe_3O_4 nano-grains [17,27]. Further investigation of the temperature dependence of the resistivity will be carried out to determine the transport mechanism, considering that increased temperature promotes thermal-activated electron hopping and overcomes the Coulomb blockade [2,17,28]. Additionally, the semiconductor-like high resistivity, as a collective behavior of the self-assembled CNPs, implies that the metallic Ag nanograins were sparely dispersed in the ferromagnetic matrix of the half-metallic Fe_3O_4 nano-grains and the Ag concentration is below the percolation threshold without forming conducting networks

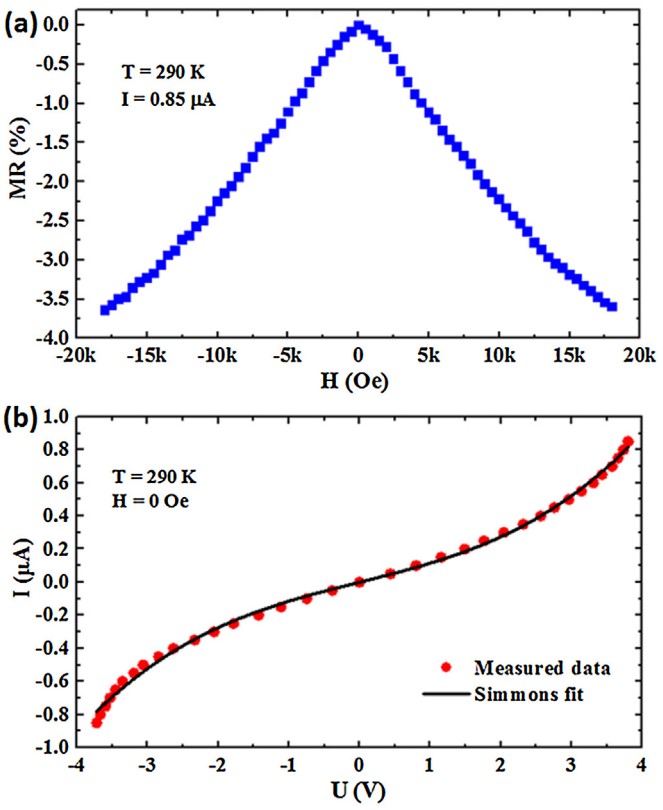

Fig. 4. (a) MR curve and (b) I–V curve of the CNP-based magnetoresistive device.

[17]. The current-voltage measurement results suggest that the CNP-assembled thin film is useful for studying the charge transport nature in nanoparticle-based granular materials with intra-particle interfaces and inter-particle barriers.

4. Conclusions

In summary, uniform thin films of Fe_3O_4-Ag CNPs were prepared by an improved self-assembly method at liquid-air interface. By further transferring such CNP-assembled thin films onto patterned substrates, CNP-based magnetoresistive devices were fabricated. The constituent CNPs in this device possess additional intra-particle interfaces and distinct inter-particle barriers, compared with their single-component counterparts. Correspondingly, an enhanced MR ratio and a non-linear I–V relation were observed in this device at room temperature. The self-assembly strategy and the thin-film fabrication procedure presented in this work can be further extended to other magnetic CNPs of different sizes or compositions, enabling the construction and integration of multi-component nanoparticles into magnetic materials and devices for spintronic applications.

Acknowledgements

This research was supported by the Seed Funding Program for Basic Research, Seed Funding Program for Applied Research and Small Project Funding Program from University of Hong Kong; ITF Tier 3 funding (ITS-104/13, ITS-214/14); and University Grants Committee of Hong Kong (AoE/P-04/08).

References

[1] G. Singh, H. Chan, A. Baskin, E. Gelman, N. Repnin, P. Král, R. Klajn, Science 345 (2014) 1149–1153.
[2] I.C. Lekshmi, R. Buonsanti, C. Nobile, R. Rinaldi, P.D. Cozzoli, G. Maruccio, ACS Nano 5 (2011) 1731–1738.
[3] V. Aleksandrovic, D. Greshnykh, I. Randjelovic, A. Fromsdorf, A. Kornowski, S.V. Roth, C. Klinke, H. Weller, ACS Nano 2 (2008) 1123–1130.
[4] T. Wen, D. Zhang, Q. Wen, H. Zhang, Y. Liao, Q. Li, Q. Yang, F. Bai, Z. Zhong, Nanoscale 7 (2015) 4906–4911.
[5] C. Jiang, C.W. Leung, P.W. Pong, Nanoscale Res. Lett. 11 (2016) 189.
[6] C. Wang, H. Yin, S. Dai, S. Sun, Chem. Mater. 22 (2010) 3277–3282.
[7] M.A. Boles, M. Engel, D.V. Talapin, Chem. Rev. 116 (2016) 11220–11289.
[8] C. Jiang, S.M. Ng, C.W. Leung, P.W. Pong, J. Mater. Chem. C 5 (2017) 252–263.
[9] J.-I. Park, Y.-w. Jun, J.-s. Choi, J. Cheon, Chem. Commun. (2007) 5001–5003.
[10] L. Jiang, X. Chen, N. Lu, L. Chi, Acc. Chem. Res. 47 (2014) 3009–3017.
[11] J.J. Giner-Casares, J. Reguera, Nanoscale 8 (2016) 16589–16595.
[12] M. Pauly, B.P. Pichon, P.-A. Albouy, S. Fleutot, C. Leuvrey, M. Trassin, J.-L. Gallani, S. Bégin-Colin, J. Mater. Chem. 21 (2011) 16018–16027.
[13] A. Dong, J. Chen, P.M. Vora, J.M. Kikkawa, C.B. Murray, Nature 466 (2010) 474–477.
[14] A. Dong, X. Ye, J. Chen, C.B. Murray, Nano Lett. 11 (2011) 1804–1809.
[15] J.-H. Hsu, S.-Y. Chen, W.-M. Chang, T. Jian, C.-R. Chang, S.-F. Lee, J. Appl. Phys. 93 (2003) 7702–7704.
[16] X. Hu, M. Xu, X. Cui, S. Zhang, Solid State Commun. 142 (2007) 595–599.
[17] J. Tang, L. Feng, J.A. Wiemann, Appl. Phys. Lett. 74 (1999) 2522–2524.
[18] Y. Kimishima, W. Yamada, M. Uehara, T. Asaka, K. Kimoto, Y. Matsui, Mater. Sci. Eng. B 138 (2007) 69–73.
[19] J.-H. Hsu, S.-Y. Chen, C.-R. Chang, J. Magn, Magn. Mater. 242 (2002) 479–481.
[20] Y. Ridelman, G. Singh, R. Popovitz-Biro, S.G. Wolf, S. Das, R. Klajn, Small 8 (2012) 654–660.
[21] J. Park, K. An, Y. Hwang, J.-G. Park, H.-J. Noh, J.-Y. Kim, J.-H. Park, N.-M. Hwang, T. Hyeon, Nat. Mater. 3 (2004) 891–895.
[22] J. Huang, Y. Sun, S. Huang, K. Yu, Q. Zhao, F. Peng, H. Yu, H. Wang, J. Yang, J. Mater. Chem. 21 (2011) 17930–17937.
[23] L. Li, A. Ruotolo, C. Leung, C. Jiang, P. Pong, Microelectron. Eng. 144 (2015) 61–67.
[24] A. Lak, J. Dieckhoff, F. Ludwig, J.M. Scholtyssek, O. Goldmann, H. Lünsdorf, D. Eberbeck, A. Kornowski, M. Kraken, F. Litterst, Nanoscale 5 (2013) 11447–11455.
[25] J. Coey, A. Berkowitz, L. Balcells, F. Putris, F. Parker, Appl. Phys. Lett. 72 (1998) 734–736.
[26] J. Petta, S. Slater, D. Ralph, Phys. Rev. Lett. 93 (2004) 136601.
[27] J.A. Wiemann, E.E. Carpenter, J. Wiggins, W. Zhou, J. Tang, S. Li, V.T. John, G.J. Long, A. Mohan, J. Appl. Phys. 87 (2000) 7001–7003.
[28] J.-H. Hsu, S.-Y. Chen, W.-M. Chang, C.-R. Chang, J. Magn. Magn. Mater. 272 (2004) 1772–1773.